Melting Behavior, Nonisothermal Crystallization Kinetics, and Morphology of PP/Nylon 11/EPDM-*g*-MAH Blends

Biaobing Wang,[1,2] Guosheng Hu,[1] Lixia Wei[1]

[1]*Shanxi Research Center of Engineering Technology for Engineering Plastics, School of Material Science and Engineering, North University of China, Taiyuan 030051, China*
[2]*Department of Grain Science and Industry, Kansas State University, Manhattan, Kansas 66506*

Received 20 June 2007; accepted 14 September 2007
DOI 10.1002/app.27485
Published online 26 November 2007 in Wiley InterScience (www.interscience.wiley.com).

ABSTRACT: The melting behavior, nonisothermal crystallization behavior, and morphology of pure polypropylene (PP) and its blends were investigated by differential scanning calorimetry and polarized optical microscopy. The nonisothermal crystallization kinetics was analyzed using the Avrami equation modified by Jeziorny and the equation combining the Avrami and Ozawa method. The surface fold free energy and the effective activation energy for both PP and its blends were obtained by Hoffman-Lauritzen theory and Vyazovkin's approach, respectively. The results showed that the presence of nylon 11 hindered the mobility of PP chains but accelerated the overall crystallization rate. The POM observation confirmed that the addition of nylon 11 decreased the spherulites size of PP matrix. © 2007 Wiley Periodicals, Inc. J Appl Polym Sci 107: 3013–3022, 2008

Key words: PP; nylon 11; melting behavior; nonisothermal crystallization kinetics; morphology

INTRODUCTION

Poly(propylene) (PP) is one of the most versatile commodity polymers for both domestic and industrial purposes because of its easy processability, relatively low cost, and especially its well-balanced physical and mechanical properties. However, in some cases, not all the characteristics of this material are suitable for common service conditions. For instance, PP exhibits poor impact resistance at low temperature and high notch sensitivity at room temperature because of its high transition temperature and high crystallinity. Therefore, toughening of PP has still attracted numerous research interests. Compounding PP with elastomers [ethylene-propylene-diene rubber (EPDM)],[1–4] ethylene-propylene rubber (EPR),[5–7] styrene-ethylene-butylene-styrene (SEBS),[8–16] etc), rigid polymer (PA6,[17–25] PA66,[26–28] LCP,[29] etc), and rigid particles ($CaCO_3$,[30–32] SiO_2[33,34]) were the three traditional approaches to improve the toughness of PP. However, the addition of elastomers often has negative effects on some properties of PP, such as the stiffness and hardness. Polypropylene (PP) and polyamide (PA) blends, especially PP/PA6 and PP/PA66 blends, have been widely studied because these blends can combine the good thermal and mechanical properties of PA and the excellent processability and resistance to moisture of PP. Since nylon 11 has excellent cold-tolerance, it was supposed that the blending of nylon 11 into PP can improve the low- temperature resistance of PP matrix. However, the different polarity between nylon 11 and PP resulted in bad compatibility, which can be generally improved by using a compatibilizer. In our lab, maleic anhydride functional copolymer compatibilizer and elasticized EPDM-*g*-MAH were chosen to compatibilize PP/PA11 system. It was noteworthy that the synergic effect of nylon 11 and EPDM-*g*-MAH on the toughness of PP occurred for the PP/nylon 11/EPDM-*g*-MAH ternary blends in our preliminary research. In contrast with that the low-temperature impact strength of pure PP was too low to be detected, the low-temperature impact strength for PP/nylon 11/EPDM-*g*-MAH ternary blends was up to 3.42 KJ/m^2. The works on the mechanical properties and morphological structure will be reported in the future article.

PP is a semicrystalline polymer. It is well understood that physical and mechanical properties of crystalline polymer depend on the morphology, crystalline structure, and degree of crystallization. During the last few years, the melting and crystallization behavior of neat PP and its blends with other polymers have been reported. Generally, the smaller the dispersed particles are the more effective is the

Correspondence to: B. Wang (bbwang@nuc.edu.cn).
Contract grant sponsor: Shanxi Science and Technology Bureau (Science and Technology Foundation for Young); contract grant number: 2006021011.
Contract grant sponsor: Science and Technology Foundation of North University of China.

nucleating agents for PP crystallization. Supaphpl et al.[35] studied the effect of calcium carbonate on the nonisothermal crystallization of s-PP, it was found that $CaCO_3$ acts as a good nucleating agent for s-PP, and the nucleating efficiency of $CaCO_3$ for s-PP was found to depend strongly on its purity, type of surface treatment, and average particle size. He and coworkers[36] investigated the nonisothermal crystallization of PP/nano-SiO_2 nanocomposite, the results showed that the nano-SiO_2 particles exhibited a remarkable heterogeneous nucleation effect in the PP matrix, and the rate of crystallization of PP/nano-SiO_2 is higher than that of pure PP. Zhang and coworkers[37] found the MPP grafted Novolac copolymer acted as a more effective heterogeneous nucleation agent of PP crystallization and accelerated the crystallization of PP meanwhile the addition of Novolac resulted in a prompt decrease in spherulite size of PP.

In this article, the nonisothermal crystallization behavior and melting behavior of pristine PP and its blends were investigated. The crystallization kinetics based on the nonisothermal crystallization of PP and blends were analyzed according to the Avrami equation modified by Jeziorny, Ozawa method, and the equation combining the Avrami and Ozawa theories. The linear growth rate and surface free energy were calculated using Huffman-Lauritzen theory, and the effective activation energy was determined through a novel approach proposed by Vyazovkin.

EXPERIMENTAL

Materials

Nylon 11 was manufactured in our laboratory, polypropylene (T30S, melt index 3.0 g/10 min) and EPDM-*g*-MAH with 1% MAH was supplied by Sinopec Qilu Company (Jinan, China) and Shanghai Sunny New Technology Development (Shanghai, China), respectively. Nylon 11 and EPDM-*g*-MAH were dried at 80°C in vacuum for at least 12 h before use.

Preparation of blends

Melt blends were obtained by using a TSSJ-25~33 twin-screw extruder (China). The three different polymer chips or powder were fed together under the screw speed at 80 rpm, and the extruding temperature at various zones was between 185 and 205°C. The extrudate was passed through a cooling water bath and were finally palletized, and then dried in vacuum over for 24 h at 100°C. For comparison, pure PP was also extruded under the above same condition.

Differential scanning calorimetry analysis

Isothermal and nonisothermal crystallization and subsequent melting behaviors were carried out using a MeTTLER DSC822^e, and the temperature was calibrated with the indium standard. All differential scanning calorimetry (DSC) experiments were performed under a nitrogen purge at a constant flow rate. Sample weights were between 2 and 3 mg. All samples were dried at 80°C under vacuum for 12 h before measurement.

DSC experiments of isothermal crystallization and subsequent melting behaviors were performed as follows: the sample was heated to 200°C at a rate of 20°C/min and held at this temperature for 10 min to eliminate any previous thermal history, and then cooled at a rate of −100°C/min to the predetermined cryatallization temperature (T_c), ranged from 118 to 128°C in steps of 2°C, and was maintained at T_c for 1 h necessary for the DSC trace to return to the calorimeter baseline. The specimens were subsequently heated to 200°C at a rate of 10°C/min.

DSC measurements of nonisothermal crystallization were performed using a similar process to the above described, and the DSC cooling traces were recorded at rates of 2.5, 5, 10, 20, and 40°C/min.

Scanning electron microscopy

The electron microscope (Hitachi S530) was employed to examine the dispersion of nylon 11 within the blends. The fractured surface was previously treated for 24 h with a boiling meta-cresol to erode nylon 11 and then coated with a thin layer of gold.

Polarized optical microscopy observation

The size of PP spherulites was studied on thin films by using a polarized optical microscopy (POM) LEICA-DMLPl, with an automatic hot-stage thermal control. A sample was sandwiched between microscope cover glasses, melted at 200°C for 5 min, and then rapidly cooled to 120°C for isothermal crystallization for 2 h.

RESULTS AND DISCUSSION

Equilibrium melting temperature

The melting behavior of the PP and its blends was investigated by reheating the isothermally crystallized samples at a heating rate of 10°C/min, and the DSC heating thermograms were presented in Figure 1. As can be seen, the melting temperature (T_m) shifted to higher temperature with increasing crystallization temperature (T_c), which was directly related to the perfection of PP crystals.

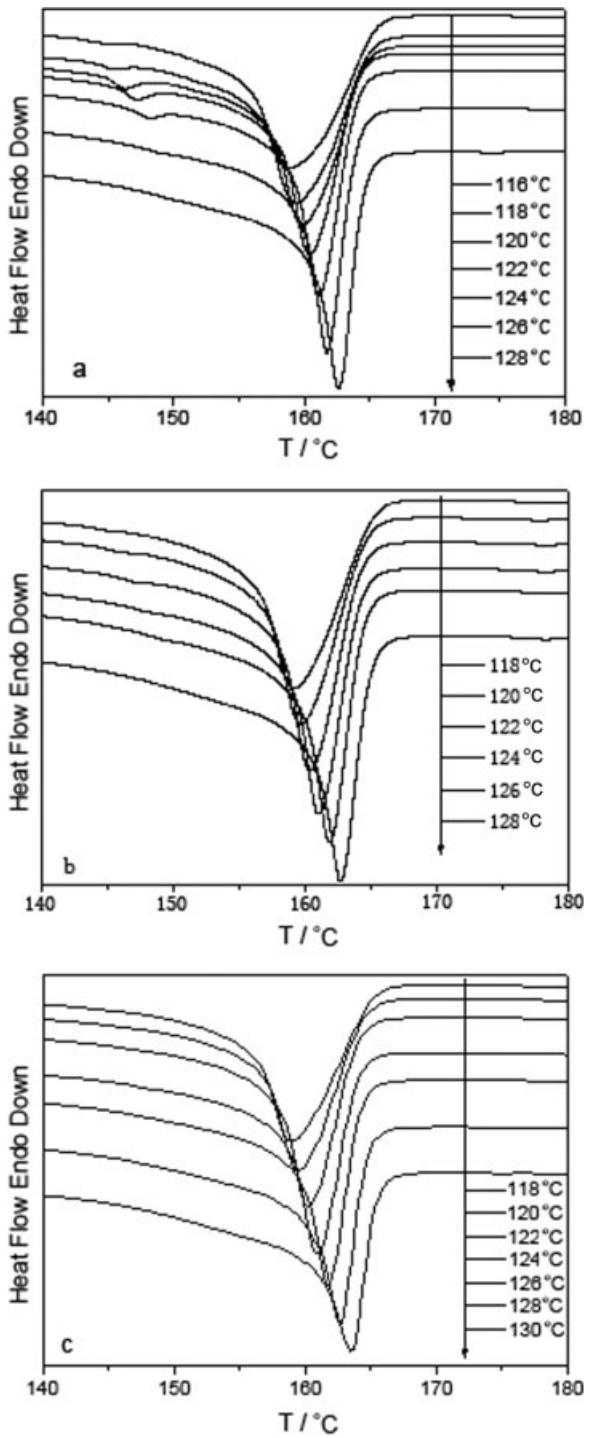

Figure 1 DSC heating thermograms of (a) PP, (b) PP/nylon 11, and (c) PP/nylon 11/EPDM-*g*-MAH blends.

Plots of T_m versus T_c are shown in Figure 2. It can be seen that T_m increased linearly with T_c in the range of T_c examined. According to the Hoffman-Weeks theory,[38] the equilibrium melting point (T_m^0) can be obtained by linear extrapolation of T_m versus T_c data to intersect the line $T_m = T_c$. Mathematically, the dependence of T_m on T_c is expressed as follows:

$$T_m = \frac{T_c}{2\beta} + T_m^0\left(1 - \frac{1}{2\beta}\right) \quad (1)$$

where β is the lamellar thickening factor which describes the growth of the lamellar thickness during

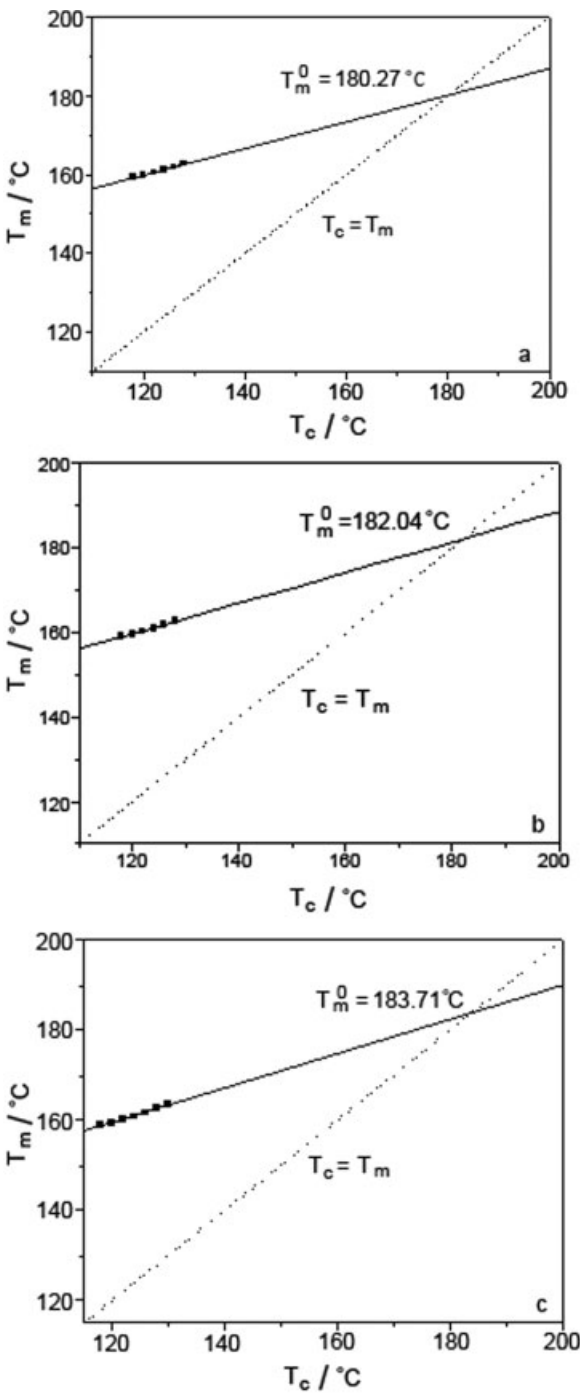

Figure 2 Melting temperature as a function of crystallization temperatures for (a) PP, (b) PP/nylon 11, and (c) PP/nylon 11/EPDM-*g*-MAH.

crystallization and is supposed to be greater than or equal to 1.

As shown in Figure 2, the values of T_m^0 can be obtained by extrapolating the least-squares fit lines of experimental data according to eq. (1) to intersect the line of $T_m = T_c$. The value of T_m^0 obtained for pristine PP, PP/nylon 11, and PP/nylon 11/EPDM-*g*-MAH was 180.27, 182.04, and 183.71°C, respectively. It was found that the T_m^0 of blends was higher than that of pristine PP, which implied that the PP crystals within blends were more perfect.

Nonisothermal crystallization kinetics

Figure 3 presented the nonisothermal crystallization curves for pristine PP, PP/nylon 11, and PP/nylon 11/EPDM-*g*-MAH blends at various cooling rates. Clearly, for all samples, the crystallization peaks and the crystallization peak temperature (T_p) shifted to low temperatures gradually with increasing of the cooling rates. Additionally, the presence of nylon 11 promoted the crystallization peak temperatures of blends in comparison with pristine PP, that is, the nylon 11 may act as the additional active substrates for the heterogeneous nucleation, resulting in that the crystallization of PP occurred at higher temperature when cooling.

The relative crystallinity, $X(t)$, at a time interval t from the initial time $t = 0$ at temperature T, can be defined as follows:

$$X(t) = \frac{\int_{T_0}^{T} \frac{dH_c(T)}{dT} dT}{\int_{T_0}^{T_\infty} \frac{dH_c(T)}{dT} dT} \quad (2)$$

where T_0 and T_∞ were the initial and final crystallization temperature, respectively. In nonisothermal crystallization, time t has the relation with temperature T as follows:

$$t = \frac{|T_0 - T|}{\phi} \quad (3)$$

where T is the temperature at time t, and ϕ is the cooling rate.

Based on the assumption that the crystallization temperature is constant, nonisothermal crystallization can be described by the Avrami equation[39,40] as follows:

$$1 - X(t) = \exp[-Z_t t^n] \quad (4)$$

or

$$\log\{-\ln[1 - X(t)]\} = n\log t + \log Z_t$$

where $X(t)$ is the relative degree of crystallinity at time t, n is the Avrami exponent that depends on the type of nucleating and growth process parameters, and Z_t is a composite rate constant involving both nucleating and growth rate parameters. Considering the nonisothermal character of the process investigated, Jeziorny[41] suggested that the parameter, Z_t, should be corrected as follows:

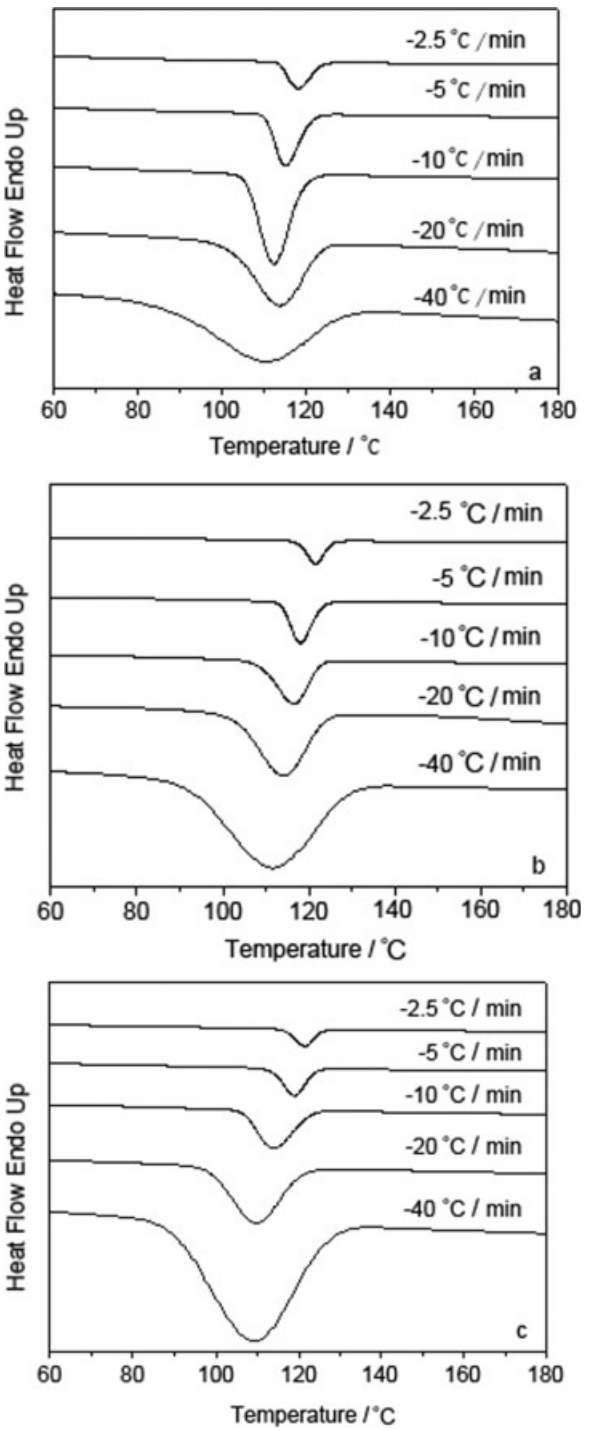

Figure 3 Nonisothermal crystallization curves of (a) PP, (b) PP/nylon 11, and (c) PP/PA11/EPDM-*g*-MAH blends at various cooling rates.

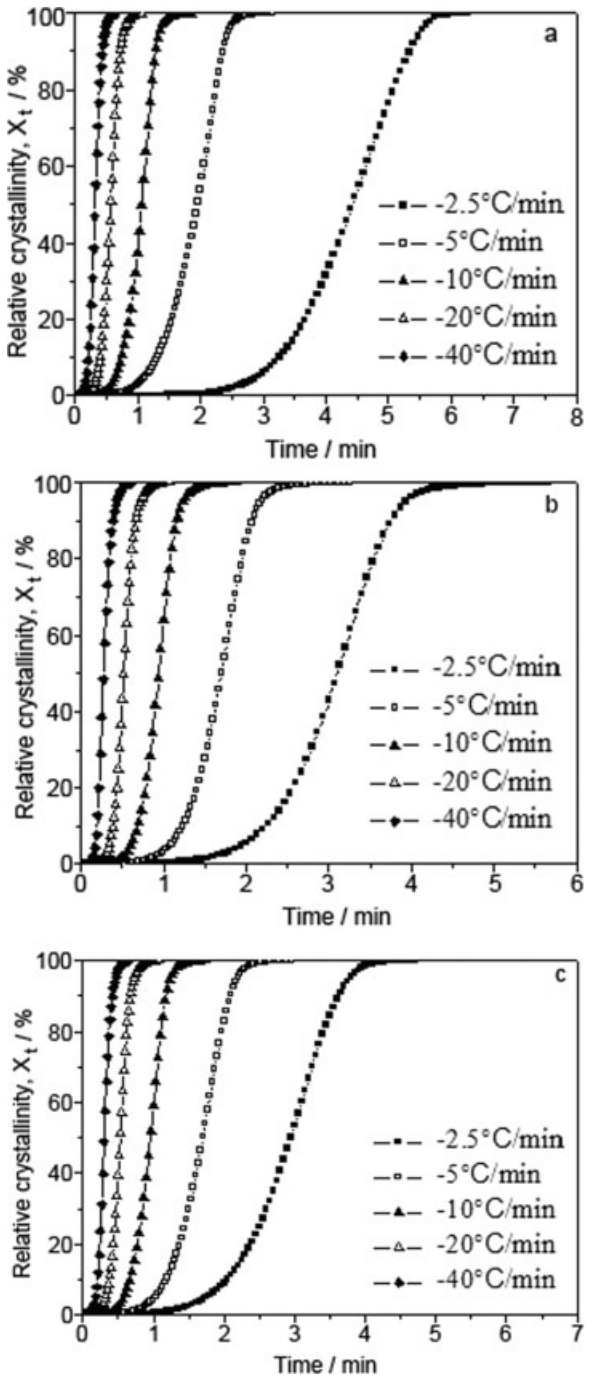

Figure 4 Relative degree of crystallinity of (a) PP, (b) PP/nylon 11, and (c) PP/nylon 11/EPDM-*g*-MAH blends as a function of time at various cooling rates.

$$\log Z_c = \frac{\log Z_t}{\phi} \tag{5}$$

Figures 4 and 5 showed a typical relative crystallinity curves and the corresponding modified Avrami plots for all samples, respectively. The results determined from Jeziorny method are summarized in Table I. As can be found, the values of n ranged from 4.53 to 6.13 for pure PP, indicating that the model of nucleation and growth during the nonisothermal crystallization process was more complex, and the nucleation model could comprise the homogeneous and heterogeneous nucleation at the same time. The values of n ranged from 4.80 to 5.73 for

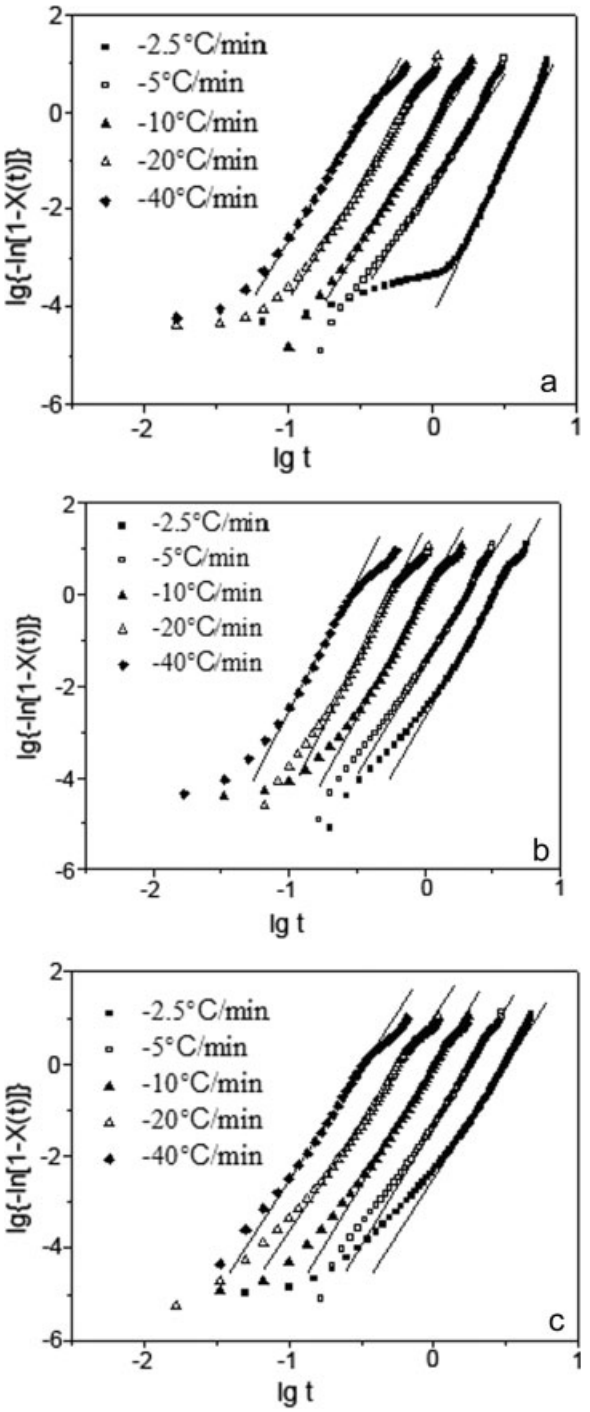

Figure 5 Plots of $\log\{-\ln[1 - X(t]\}$ versus $\log t$ for (a) PP, (b) PP/nylon 11, and (c) PP/nylon 11/EPDM-*g*-MAH blends.

TABLE I
Nonisothermal Crystallization Kinetics Parameters Determined from Jeziorny Method and Mo Method for Pristine PP and its Blends

Sample	ϕ (°C/min)	n	Z_c	$t_{1/2}$ (min)	T_p (°C)	$X(T)$ (%)	$F(T)$	α
Pristine PP	2.5	6.13	0.02	4.41	118.1	20	8.823	1.040
	5	4.53	0.50	1.97	114.9	40	10.540	1.065
	10	4.62	0.91	1.07	112.8	60	11.997	1.088
	20	4.65	1.10	0.58	110.3	80	13.377	1.093
	40	4.88	1.14	0.32	106.9			
PP/nylon11	2.5	5.19	0.08	3.11	121.1	20	7.345	1.121
	5	4.80	0.49	1.70	118.2	40	8.712	1.146
	10	5.28	0.99	0.92	115.4	60	9.792	1.156
	20	5.73	1.18	0.51	112.9	80	10.982	1.176
	40	5.41	1.18	0.27	109.9			
PP/nylon 11/EPDM-*g*-MAH	2.5	4.91	0.10	2.94	120.9	20	7.464	1.189
	5	5.18	0.54	1.7	118.2	40	8.812	1.214
	10	5.08	0.99	0.95	114.9	60	9.954	1.221
	20	4.71	1.13	0.53	111.6	80	11.233	1.221
	40	5.03	1.15	0.29	108.2			

PP/nylon 11 and 4.71 to 5.18 for PP/nylon 11/EPDM-*g*-MAH blends, showing that the crystallization mechanism was not affected by the variation of the blend composition. However, the modified crystallization rate constant Z_c of blends increased to some extent in contrast to that of pristine PP, indicating that nylon 11 may accelerate the nonisothermal crystallization process of PP matrix, which were also reflected by the reduction on the half crystallization time, $t_{1/2}$.

Assuming that the crystallinity is correlated to both the cooling rate and the crystallization time and consequently for particular crystallinity, these two parameters can be derived by combining the Avrami and Ozawa equations, Mo and coworkers[42] developed a novel kinetic approach by combining the Avrami equation with the Ozawa equation to describe exactly the nonisothermal crystallization process.

The Avrami equation as modified by Ozawa in double logarithmic form is expressed as follows[43]:

$$\log\{-\ln[1 - X(T)]\} = \log K(T) - m\log \phi \qquad (6)$$

where $K(T)$ is the function of cooling rate which related to the overall crystallization rate, and m is the Ozawa exponent that depends on the dimension of crystals growth.

Therefore, combining the eqs. (4) and (6), the following equation were obtained at a given crystallinity degree,

$$\log Z_t + n\log t = \log K(T) - m\log \phi$$

$$\log \phi = \frac{1}{m}\log\left[\frac{K(T)}{Z_t}\right] - \frac{n}{m}\log t$$

$$\log \phi = \log F(T) - \alpha\log t \qquad (7)$$

where $F(T) = [K(T)/Z_t]^{1/m}$ is the necessary value of cooling rate to reach a certain degree of crystallinity at unit crystallization time, and $\alpha = n/m$. According to eq. (7), at a given degree of crystallinity, plots of $\log \phi$ versus $\log t$ exhibited a good linear relationship, as shown in Figure 6. Thus, the nice linearity of those curves revealed that the Mo model provided a satisfactory description to the nonisothermal crystallization for both the pristine PP and its blends. Values of α and $F(T)$, as also listed in Table I, were calculated from the slope and intercept of these lines, respectively. It can be seen that the values of $F(T)$ increased with increasing relative degree of crystallinity, indicating that a higher cooling rate should be adopted to obtain a higher degree of crystallinity at unit crystallization time. Moreover, it is obvious that for a certain degree of crystallinity, the values of $F(T)$ for the blends was smaller than that for the pristine PP, that is, approaching to the identical relative degree of crystallinity, the blends require lower cooling rate. In other words, the blends showed a higher crystallization rate than pristine PP, which was in agreement with the results from Jeziorny method.

Linear growth rate and surface free energy

The Huffman-Lauritzen theory[44] suggests that the linear growth rate, G, depends on temperature, T, as follows:

$$G = G_0 \exp\left(\frac{-U^*}{R(T_c - T_\infty)}\right)\exp\left(\frac{-K_g}{T_c\Delta T f}\right)$$
$$\ln G + \frac{-U^*}{R(T_c - T_\infty)} = \ln G_0 - \frac{K_g}{T_c\Delta T f} \qquad (8)$$

where G_0 is the pre-exponential factor, U^* is the activation energy of the segmental jump, $\Delta T = T_m^0 - T_c$

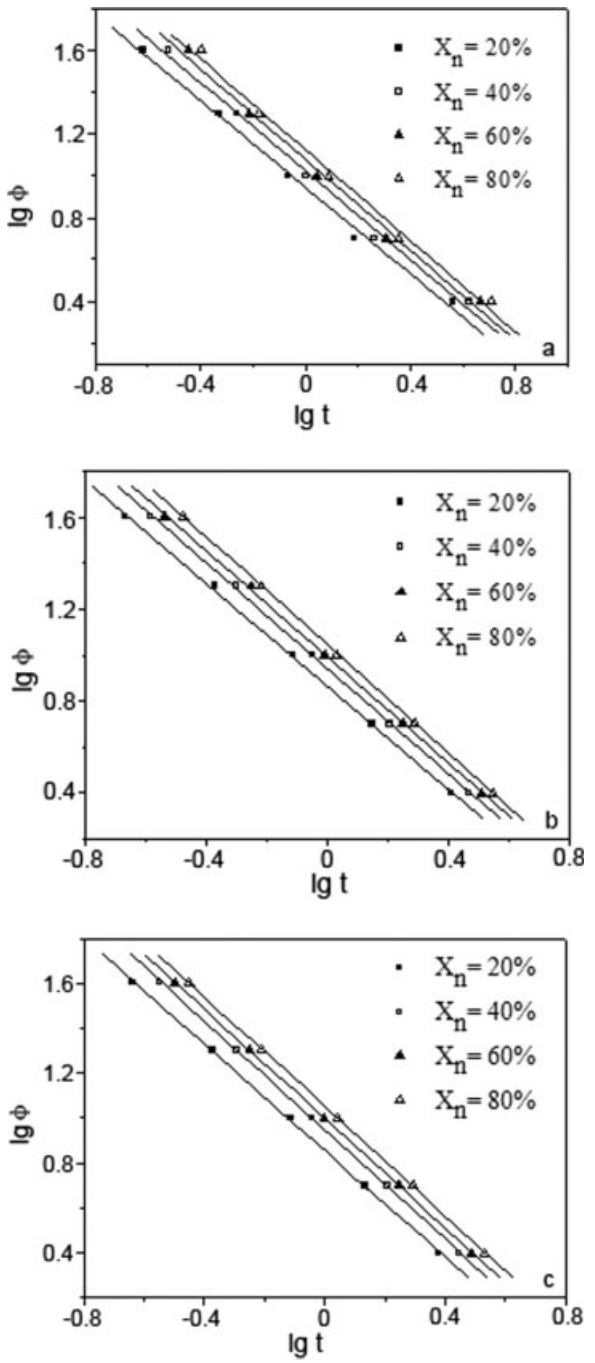

Figure 6 Plots of log ϕ versus log *t* for (a) PP, (b) PP/nylon 11, and (b) PP/nylon 11/EPDM-*g*-MAH blends.

is the under cooling, $f = 2T_c/(T_m^0 + T_c)$ is the correction factor, and T_∞ is a hypothetical temperature where motion associated with viscous flow ceases that is usually taken 30 K below the glass transition temperature T_g. The kinetic parameter, K_g, has the following form:

$$K_g = \frac{nb\sigma\sigma_e T_m^0}{\Delta h_f k_B} \tag{9}$$

where b is the distance between two adjacent fold planes, σ and σ_e are the lateral and fold surface free energy, k_B is the Boltzmann constant, Δh_f is the heat of fusion per unit volume of crystal, and n takes the value 4 for crystallization regimes I and II and 2 for regime II. In this work, the crystallization regime II was observed and n took the value 2. The value of U^* was set to the constant value 6300 J/mol, which was suitable for most polymers. The values of K_g for pristine PP, PP/nylon 11, and pp/nylon 11/EPDM-*g*-MAH blends were obtained from DSC data on isothermal crystallization using eq. (9), in which the values of G and G_0 were substituted with $(1/t_{1/2})$ and $(1/t_{1/2})_0$, respectively.[45] The plots of $\ln G + U^*/R(T - T_\infty)$ versus $1/T_c\Delta Tf$ are shown in Figure 7. The values of K_g for pristine PP, PP/nylon 11, and PP/nylon 11/EPDM-*g*-MAH were calculated to be 4.362×10^5 K^2, 4.796×10^5 K^2, and 4.596×10^5 K^2. The values of K_g can be used to evaluate the product $\sigma\sigma_e$ from eq. (9). Using the literature[46] values of b = 6.56 Å and $\Delta h_f = 1.34 \times 10^8$ J/m^3, the values of $\sigma\sigma_e$ were 6.68×10^{-4} J^2/m^4 for pristine PP, 7.43×10^{-4} J^2/m^4 for PP/nylon 11 blend, and 7.09×10^{-4} J^2/m^4 for PP/nylon 11/EPDM-*g*-MAH blend. σ was often estimated as follows:

$$\sigma = 0.11\Delta h_f \sqrt{a_0 b_0} \tag{10}$$

where a_0 and b_0 are the parameters of the PP unit cell. Using a_0 = 6.65 Å and b_0 = 20.96 Å, σ was calculated to be 1.74×10^{-2} J/m^2. Substitution of this value into $\sigma\sigma_e$, it can be obtained that the fold surface free energy $\sigma_e = 3.84 \times 10^{-2}$ J/m^2 for pristine PP, 4.27×10^{-2} J/m^2 for PP/nylon 11 and 4.07×10^{-2} J/m^2 for PP/nylon 11/EPDM-*g*-MAH blends. It was obvious that the fold surface free energy of the blends was higher than that of the pristine PP, inferring that the presence of nylon 11 hindered the mobility of PP chains.

Effective activation energy

Considering the fact that the rate of crystallization was generally determined by the rates of nucleation and nuclei growth, whose activation energies were likely to be different, Vyazovkin and Sbirrazzuoli[47] proposed a new approach deduced from the Hoffman-Laruitzen theory eq. (8) to evaluate the effective activation energy, E_α, which was a function of temperature. The E_α can be represented as eq. (11).

$$E_\alpha(T) = U^* \frac{T^2}{(T - T_\infty)^2} + K_g R \frac{T_m^{0^2} - T^2 - T_m^0 T}{(T_m^0 - T)^2 T} \tag{11}$$

This method has been used to calculate K_g and U^* parameters for the Hoffman-Lauritzen theory via

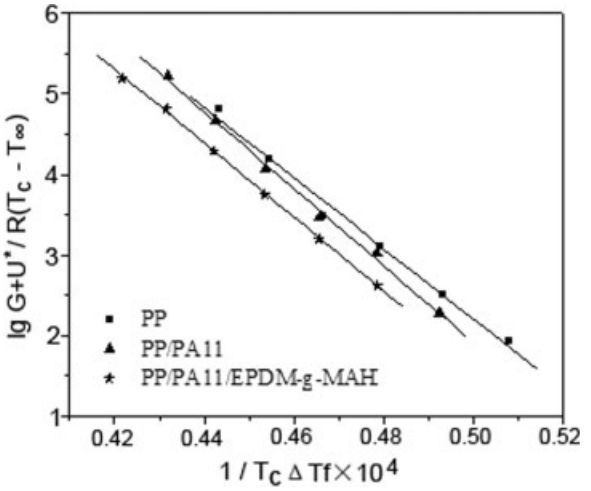

Figure 7 Plots of $\ln G + U^*/R(T_c - T_\infty)$ versus $1/T_c\Delta Tf$ for (a) PP, (b) PP/nylon 11, and PP/nylon 11/EPDM-*g*-MAH blends.

applying an isoconversional method to DSC data on nonisothermal crystallization. In this article, the values of K_g obtained from eq. (8) were used to estimate the E_α for PP and its blends.

Substitution of K_g values into eq. (11) permitted estimation of the effective activation energy, E_α, and the curves of E_α versus T for PP and its blends were shown in Figure 8. The values of E_α were negative, indicating that the rate of crystallization increased with decreasing temperatures. The absolute values of E_α for blends were higher than that of pure PP, which revealed that PP molecular segments required more energy to rearrange in the presence of nylon 11, since the nylon 11 might hinder the mobility of chain segments. Additionally, the absolute values of E_α for PP/nylon 11 was greater than that for PP/nylon 11/EPDM-*g*-MAH, it was indicated that the addition of EPDM-*g*-MAH alleviated the inhibition of nylon 11 on the mobility of PP chains. The anhydride units of EPDM-*g*-MAH reacted readily with the amine end groups of nylon 11 to form block or graft copolymers,[48,49] which thus became compatible with PP. Therefore, the copolymers diffused into the PP matrix carrying neighboring nylon 11 chains into the PP matrix during the melting blend. And vice versa, the PP macromolecules readily diffused into the nylon 11 heterogeneous nucleating agent during the cooling crystallization process. The improved compatibility between PP and nylon 11 in the presence of EPDM-*g*-MAH were confirmed by the reduced domain size of nylon 11, as can be seen from scanning electron microscopy (SEM) images (illustrated in Fig. 9).

Paradoxically, the experimental results showed that the addition of nylon 11 into PP hindered the mobility of PP macromolecular chains and the growth of spherulites but increased the overall crystallization rate. As we all know, the overall crystallization rate included both the nucleation rate and the growth rate, while their temperature-dependence was different. Generally, the heterogeneous nucleation can occur under higher crystallization temperature, but the homogeneous nucleation occurs only in

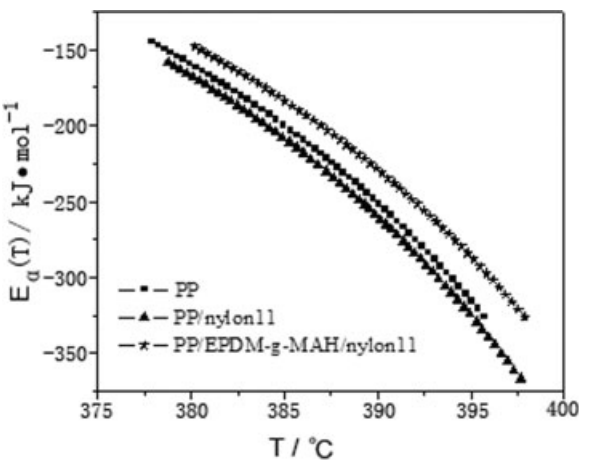

Figure 8 Plots of E_α versus T for (a) PP, (b) PP/nylon 11 and PP/nylon 11/EPDM-*g*-MAH blends.

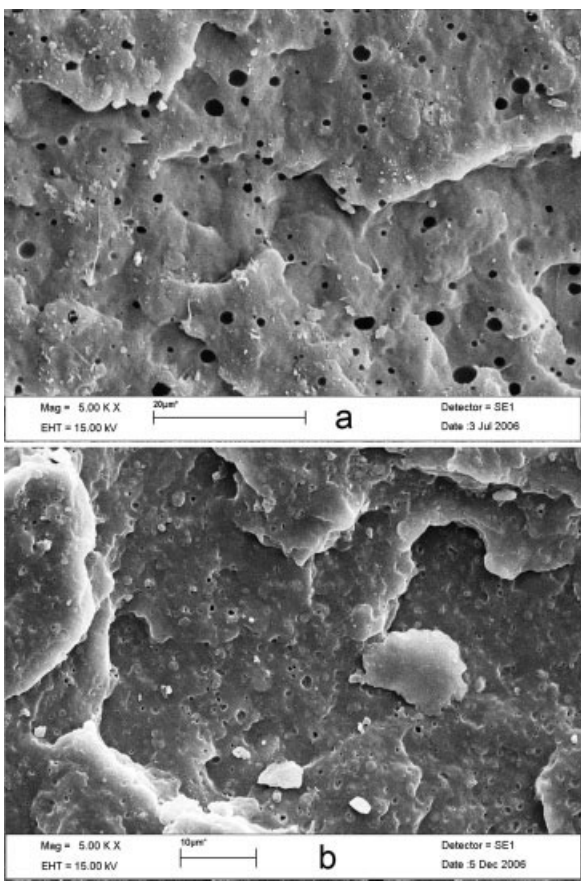

Figure 9 SEM images for (a) PP/nylon 11, and (b) PP/nylon 11/EPDM-*g*-MAH blends.

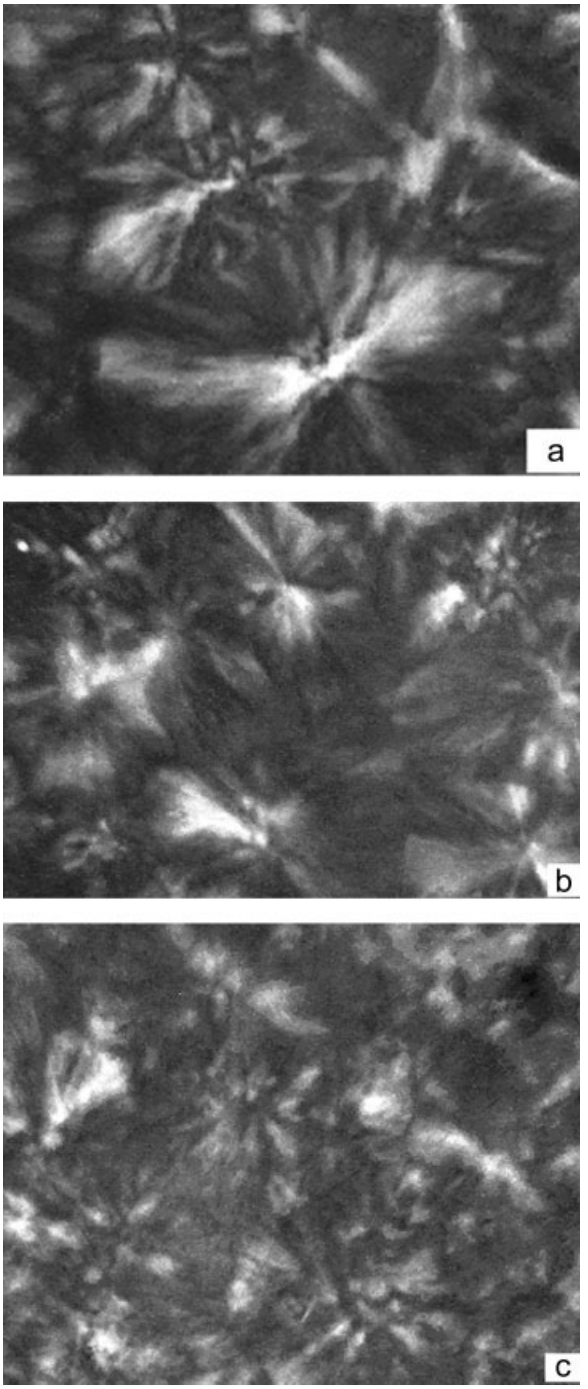

Figure 10 POM micrographs of (a) PP, (b) PP/nylon 11, and (c) PP/nylon 11/EPDM-*g*-MAH blends which isothermal crystallized at 120°C for 2 h in the magnification of 600.

the case of low crystallization temperature. On the other hand, the growth of spherulites depended on the diffusion capability and regular pileup velocity of the chain into the crystal nucleus.[50] In the system we investigated that, nylon 11 acted as heterogeneous nucleating agent and facilitated greatly the nucleation rate, it thus promoted the overall crystallization rate. On the other hand, it inhibited the diffusion of PP chain into the crystal nucleus, and therefore hindered the growth of spherulites.

Morphology

The POM was used to characterize the crystallization morphology of polymer and its composites. Figure 10 gave the POM micrographs of PP and its blends that were isothermally crystallized at 120°C for 2 h. As shown in Figure 10(a), the pure PP exhibited the common spherulites with sharp and clear birefringence. Obviously, in Figure 10, it can be observed that the spherulites of blends became smaller than that of pure PP and are distorted and interlaced with each other. It was attributed to the nucleating effect of nylon 11. Moreover, in comparison with PP/nylon 11 binary blends, the spherulites size of PP/nylon 11/EPDM-*g*-MAH blends was much smaller than that of PP/nylon 11 binary blends. When the EPDM-*g*-MAH was added, the interfacial adhesion between PP and nylon 11 was improved, which resulted in the enhanced dispersion and nucleation effect of nylon 11. Therefore, more heterogeneous nucleation sites would form within PP/nylon 11/EPDM-*g*-MAH blends, and the spherulites size became smaller.

CONCLUSIONS

In conclusion, it was found that the equilibrium melting point for pristine PP was lower than that of blends, implying that the crystal perfection was increased on blending. The obtained data for the nonisothermal crystallization could be analyzed properly by the Avrami equation modified by Jeziorny and the equation combining the Avrami and Ozawa theories. The results showed that the addition of nylon 11 accelerated the overall nonisothermal crystallization rate of PP matrix as nylon 11 might act as heterogeneous nucleating agent, but it hindered the mobility of PP chains and decreased the spherulites size of PP. It was also found that the cooling rate required to achieve identical relative degree of crystallinity was smaller for the blends than pristine PP. The surface free energy of the blends was higher than that of pristine PP, which is attributed to hindrance of mobility of PP chains caused by nylon 11 chains.

References

1. Jiang W.; Yu, D. H.; An, L. J. J Polym Sci Part B: Polym Phys 2004, 42, 1433.
2. Wang, W. Z.; Wu, Q. H.; Qu, B. J. Polym Eng Sci 2003, 43, 1798.
3. Jiang, W.; Tjong, S. C.; Li, R. K. Y. Polymer 2000, 41, 3479.

4. Wang, C.; Chang, C. I. J Appl Polym Sci 2000, 75, 1033.
5. Yazdani-Pedram, M.; Quijada, R.; Lopez-Manchado, M. A. Macromol Mater Eng 2003, 288, 875.
6. Kotter, I.; Grellmann, W.; Koch, T.; Seidler, S. J Appl Polym Sci 2006, 100, 3364.
7. Dubnikova, I. L.; Berezina, S. M.; Antonov, A. V. J Appl Polym Sci 2002, 85, 1911.
8. Gupta, A. K.; Purwar, S. N. J Appl Polym Sci 1984, 29, 1079.
9. Gupta, A. K.; Purwar, S. N. J Appl Polym Sci 1984, 29, 1595.
10. Gupta, A. K.; Purwar, S. N. J Appl Polym Sci 1984, 29, 3513.
11. Gupta, A. K.; Purwar, S. N. J Appl Polym Sci 1984, 31, 535.
12. Matsuda, Y.; Mano, T. Polym Eng Sci 2005, 45, 1630.
13. Abreu, F. O. M. S.; Forte, M. M. C.; Liberman, S. A. J Appl Polym Sci 2005, 95, 254.
14. Setz, S.; Stricker, F.; Kressler, J.; Duschek, T.; Mulhaupt, R. J Appl Polym Sci 1996, 59, 1117.
15. Bassani, A.; Pessan, L. A.; Hage, E. J Appl Polym Sci 2001, 82 2185.
16. Wilkinson, A.; Clemens, M. L.; Harding, V. M. Polymer 2004, 45, 5239.
17. Jafari, S. H.; Gupta, A. K. J Appl Polym Sci 1999, 71, 1153.
18. Jafari, S. H.; Gupta, A. K.; Rana, S. K. J Appl Polym Sci 2000, 75, 1769.
19. Bai, S. L.; G'Sell, C.; Hiver, J. M.; Mathieu, C. Polymer 2005, 46, 6437.
20. Seo, Y.; Ninh, T. H. Polymer 2004, 45, 8573.
21. Laurens, C.; Creton, C.; Leger, L. Macromolecules 2004, 37, 6814.
22. Bai, S. L.; Wang, G. T.; Hiver, J. M.; G'Sell, C. Polymer 2004, 45, 3063.
23. Tseng, F. P.; Lin, J. J.; Tseng, C. R.; Chang, F. C. Polymer 2001, 42, 713.
24. Tucker, J. D.; Lee, S. Y.; Einsporn, R. L. Polym Eng Sci 2000, 40, 2577.
25. Ohlsson, B.; Hassander, H.; Tornell, B. Polymer 1998, 39, 6705.
26. Huang, W. Y.; Shen, J. W.; Chen, X. M. J Mater Sci 2003, 38, 541.
27. Sacchi, A.; Di Landro, L.; Pegoraro, M.; Severini, F. Eur Polym J 2004, 40, 1705.
28. Krache, R.; Benachour, D.; Potschke, P. J Appl Polym Sci 2004, 94, 1976.
29. Bualek-Limcharoen, S.; Samran, J.; Amornsakchai, T.; Meesiri W. Polym Eng Sci 1999, 39, 312.
30. Chan, C. M.; Wu, J. S.; Li, J. X.; Cheung, Y. K. Polymer 2002, 43, 2981.
31. Zhang, L.; Li, C. Z.; Huang, R. J Polym Sci Part B: Polym Phys 2004, 42, 1656.
32. Yang, K.; Yang, Q.; Li, G. X.; Sun, Y. J.; Feng, D. C. Mater Lett 2006, 60, 805.
33. Wu, W.; Wagner, M. H.; Xu, Z. D. Coll Polym Sci 2003, 281, 550.
34. Wu, C. L.; Zhang, M. Q.; Rong, M. Z.; Lehmann, B.; Friedrich, K. Polym Polym Comp 2003, 11, 559.
35. Supaphpl, P.; Harnsiri, W.; Junkasem, J. J Appl Polym Sci 2004, 92, 201.
36. Qian, J.; He, P.; Nie, K. J Appl Polym Sci 2004, 91, 1013.
37. Cui, L.; Wang, S.; Zhang, Y.; Zhang, Y. J Appl Polym Sci 2007, 105, 379.
38. Hoffman, D.; Weeks, J. J. J Chem Phys 1962, 37, 1723.
39. Avrami, M. J Chem Phys 1939, 7, 1103.
40. Avrami, M. J Chem Phys 1940, 8, 212.
41. Jeziorny, A. Polymer 1978, 19, 1142.
42. Liu, T.; Mo, Z.; Wang, S.; Zhang, H. Polym Eng Sci 1997 37, 568.
43. Ozawa, T. Polymer 1971, 12, 150.
44. Hoffman, D. J.; Davis, G. T.; Lauritzen, J. I. In Treatise on Solid State Chemistry; Hammay, N. B., Ed.; Plenum: New York, 1976; Vol. 3, p 497.
45. Lu, X.; Hay, J. N. Polymer 2001, 42, 9423.
46. Ma, J.; Qi, Z.; Li, G.; Hu, Y. L. Acta Polym Sin 2001, 5, 589.
47. Vyazovkin, S.; Sbirrazzuoli, N. Macromol Rapid Commun 2004, 25, 733.
48. Hu, G.; Wang, B.; Zhou, X. Mater Lett 2007, 58, 3457.
49. Hu, G.; Wang, B.; Zhou, X. Polym Int 2005, 54, 316.
50. He, M. Polymer Physics; Fudan University Press: Shanghai, 1990.